



## Discovery of a novel class of triazolones as Checkpoint Kinase inhibitors—Hit to lead exploration

Vibha Oza<sup>a,\*</sup>, Susan Ashwell<sup>a</sup>, Patrick Brassil<sup>a</sup>, Jason Breed<sup>b</sup>, Chun Deng<sup>a</sup>, Jay Ezhuthachan<sup>a</sup>, Heather Haye<sup>b</sup>, Candice Horn<sup>a,†</sup>, James Janetka<sup>a,‡</sup>, Paul Lyne<sup>a</sup>, Nicholas Newcombe<sup>b</sup>, Ludo Otterbien<sup>b</sup>, Martin Pass<sup>b</sup>, Jon Read<sup>b</sup>, Sian Roswell<sup>b</sup>, Mei Su<sup>a</sup>, Dorin Toader<sup>a</sup>, Dingwei Yu<sup>a</sup>, Yan Yu<sup>a</sup>, Anna Valentine<sup>b</sup>, Peter Webborn<sup>b</sup>, Ann White<sup>b</sup>, Sonya Zabudoff<sup>a,§</sup>, Xiaolan Zheng<sup>a</sup>

<sup>a</sup>AstraZeneca R&D Boston, 35 Gatehouse Drive, Waltham, MA 02451, USA

<sup>b</sup>AstraZeneca R&D Alderley Park, Cheshire, Macclesfield SK10 4TG, UK

### ARTICLE INFO

#### Article history:

Received 11 June 2010

Revised 2 July 2010

Accepted 6 July 2010

Available online 29 July 2010

#### Keywords:

Triazolones

CHK1

Checkpoint Kinase inhibitors

### ABSTRACT

Checkpoint Kinase-1 (Chk1, CHK1, CHEK1) is a Ser/Thr protein kinase that mediates cellular responses to DNA-damage. A novel class of Chk1 inhibitors, triazoloquinolones/triazolones (TZ's) was identified by high throughput screening. The optimization of these hits to provide a lead series is described.

© 2010 Elsevier Ltd. All rights reserved.

Checkpoint Kinase-1 (Chk1, CHK1, CHEK1) is a Ser/Thr protein kinase that mediates the cellular response to DNA-damage. Upon DNA-damage, Chk1 is activated by ATM and ATR kinases, which phosphorylate residues Ser-317 and/or Ser-345. Chk1 mediated signaling ultimately leads to S-phase or G2/M cell cycle arrest primarily driven by Cdk inhibition. Consequently Chk1 inhibition would abrogate this arrest, and therefore permit a cell with damaged DNA to continue through the cell cycle, ultimately resulting in mitotic catastrophe and/or apoptosis.<sup>1,2</sup> Therefore, Chk1 inhibitors have been highly sought after based on their potential to enhance the efficacy of either chemo- or radio-therapeutic treatments.<sup>2</sup> Here, we report the identification and SAR of a new class of Chk1 inhibitors, the triazolones (TZs).

Early work with the staurosporine analog, UCN-01 identified it as a potent Chk1 and Chk2 inhibitor (IC<sub>50</sub> 10 nM for each).<sup>3</sup> However, it also potently inhibits various other kinases, including a number of the cyclin-dependent kinases. Thus, the clinical effects of this agent cannot be presumed to predict the effects that will be seen with inhibitors with greater specificity.

The observed potentiation of the effects of DNA-damaging agents by UCN-01 is, however, considered to be due to the ability

of the compound to inhibit Chk1, and hence abrogate cell cycle arrest.<sup>4</sup>

It is known that UCN-01 binds to Chk1 in the same manner that it binds to CDK2, PDK1, and PKC.<sup>5</sup>

Due to the rather promiscuous nature and high molecular weight of staurosporine and related analogs such as UCN-01, novel scaffolds were sought using a HTS screen using a Chk1 scintillation proximity assay. This screen identified several structural classes of Chk1 inhibitor (Fig. 1). The three major series identified were thiophene carboxamide ureas (exemplified by **1**; IC<sub>50</sub> 0.15 μM), pyrazoles (exemplified by **2**; IC<sub>50</sub> 0.6 μM), and triazolones (exemplified by **3**; IC<sub>50</sub> 0.8 μM). All the three chemotypes were pursued as lead series.<sup>6</sup>

Initial selectivity screening of the parent triazolone **3** showed it to be surprisingly selective for Chk. When screened against the

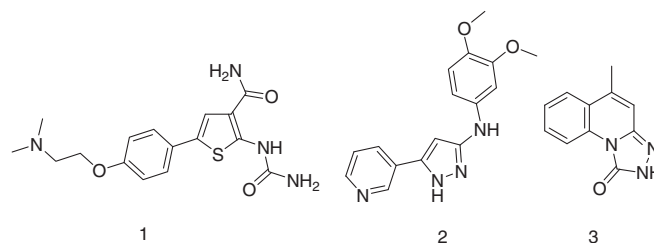


Figure 1. Chk-1 inhibitors identified from high-throughput screening.

\* Corresponding author. Tel.: +1 781 839 4448; fax: +1 781 839 4630.

E-mail address: [Vibha.Oza@astrazeneca.com](mailto:Vibha.Oza@astrazeneca.com) (V. Oza).

† Present address: Lilly, Indianapolis, IN, USA.

‡ Present address: Washington University, School of Medicine, USA.

§ Present address: Pfizer, San Diego, CA, USA.

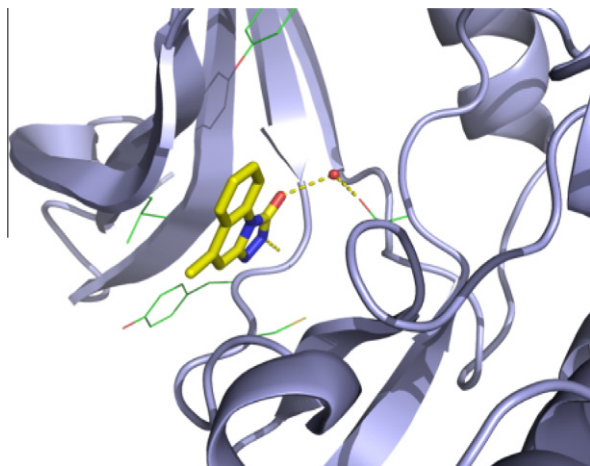


**Figure 2.** Crystal structure of TZ **3** in Chk-1 kinase domain. The TZ makes the canonical H-bond interactions with the backbone NH of C87 and the backbone carbonyl of Y86. In addition a bridging water is trapped between **3** and the side chain of S147 (PDB ID 2x8d). Picture created using PYMOL.<sup>13</sup>

Dundee panel of kinases, compound **3** showed no significant activity at 10  $\mu$ M other than Chk1.<sup>7</sup>

The initial hit **3** was therefore co-crystallized with Chk1 protein<sup>8</sup> to help guide SAR studies. The structure shown in Figure 2 revealed that the nitrogens of the five-membered ring of the triazolone make a donor–acceptor interaction with the backbone Cys<sup>87</sup> and Glu<sup>85</sup> residues in the hinge region, with the carbonyl directed toward the selectivity pocket, and trapping a water molecule that bridges to Ser<sup>147</sup>. The 4-methyl group is directed into the solvent channel of the kinase domain. Therefore, it was deduced that there was the potential to introduce additional interactions with the protein (e.g., by accessing the solvent channel, P-loop or sugar binding pocket) by additionally derivatizing the triazolone core.

It was found that the 4-methyl substituent was desirable both for retention of potency as well as ease of synthesis (see Scheme 1). Thus, holding the 4-methyl group constant, additional substituents were added in an attempt to access the sugar-binding pocket. These studies suggested that C6 and C7 substituted 4-methyl triazolones showed the most promise for delivering potent compounds. C6 and C7 disubstituted compounds, however, were mostly only moderately to weakly potent in the enzyme assay,<sup>2</sup> and were found to be devoid of cellular activity.<sup>2,9</sup> Thus efforts focused on generating a library of 7-substituted aryltriazolones that was prepared via Suzuki coupling in a multiple parallel synthesis (MPS) format. The choice of aryl boronic acids was governed by both structural information suggesting the potential to form interactions in the sugar-binding pocket or P-loop of Chk1 kinase and commercial availability. The synthetic scheme was designed to

be amenable to library synthesis as the penultimate product could readily be prepared on a large scale using the synthetic scheme outlined in Scheme 1.

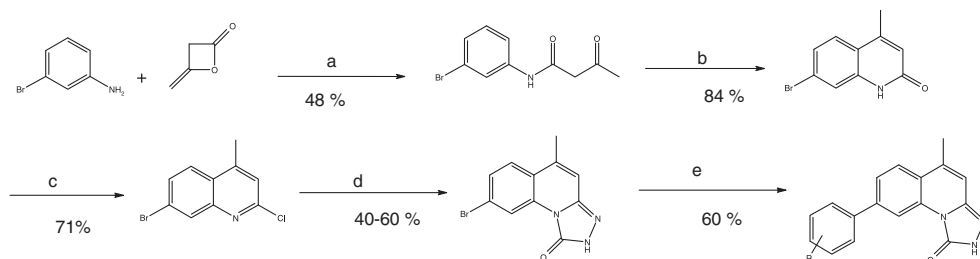
7-Bromo-2-chloro-4-methyl-quinoline was prepared in three steps from commercially available reagents by the method of Roth and co-workers.<sup>10</sup> Reaction of 3-bromoaniline with diketene in refluxing toluene led to the formation of 3-bromoacetoacetanilide in 48% yield. Cyclization of 3-bromoacetoacetanilide in concentrated H<sub>2</sub>SO<sub>4</sub> gave 7-bromo-4-methyl-2(1H)-quinoline in 84% yield. Chlorination of this quinolone was accomplished by refluxing in POCl<sub>3</sub> and the desired compound obtained in 84% yield. The route to the penultimate intermediate, 7-bromo-4-methyl-triazolone was developed using microwave chemistry. This essentially involved heating a suspension of 7-bromo-chloroquinolone in ethanol with ethyl carbazate in the presence of catalytic amounts of 4 M HCl in dioxane at 170 °C for 20 min to form 7-bromo-4-methyl-triazolone in 60% yield.

In order to identify the optimal distance between the aryl ring and the polar substituent necessary for interactions with the sugar binding pocket, two subsets of compounds were generated with and without a methylene spacer as shown in Tables 1 and 2. Additionally, the synthesis of C6 substituted matched pairs was undertaken. The C6 substituted compounds were consistently lower in potency<sup>11</sup> than their C7 substituted counterparts (data for selected compounds shown in Tables 1 and 2). Compounds **4a** and **4b** were synthesized with the intent to derivatize the more potent of the two further in order to access the sugar binding pocket.

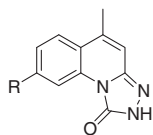
Compound **4a** was co-crystallized with Chk1 enzyme,<sup>8</sup> and confirmed the design hypotheses of generating interactions with residues in the vicinity of the ribose binding region of the kinase domain. The phenolic group was found to make a hydrogen bonding interaction with the side chain of Glu<sup>91</sup>, as depicted in Figure 3.

As hypothesized, aryl-substituted polar groups appeared to make key interactions with the sugar-binding pocket resulting in an increase in potency by about 10-fold compared to the parent triazolone **3**. From the initial library efforts, it was found that derivatization of the TZ core with 3-hydroxyphenyl moiety **4a** was tolerated and resulted in a 190 nM compound conferring about a fourfold boost in potency relative to the parent compound **3**.

4-Hydroxyphenyl substitution on the other hand yielded a very potent compound (**4b**, IC<sub>50</sub> 10 nM). Methylation of the phenolic group of **4b**, however, resulted in an approximate 50-fold drop in potency (**5**, IC<sub>50</sub> 520 nM). Encouraged by this observation, additional ether-linked analogs were generated as exemplified by **6** and **7**, both bearing a terminal amino group to access the sugar binding pocket. This yielded even more potent compounds, **6** and **7** having IC<sub>50</sub> values of 0.01 and 0.03  $\mu$ M, respectively. The 4-cyano (**15**) and 4-methylsulfoxide (**8**) aryl substituents also gave a modest increase of about eightfold. Additional 4-substituents included derivatized 4-carboxy and reverse amide moieties on the aryl ring. Both substitution patterns appear to be tolerated with specific analogs having improved potencies over the original HTS hit **3** that



**Scheme 1.** Synthesis of 7-bromo-4-methyltriazolone. Reagents and conditions: (a) reflux, 6 h; (b) concd H<sub>2</sub>SO<sub>4</sub>, 1 h; (c) POCl<sub>3</sub> reflux, 3 h; (d) NH<sub>2</sub>NHCOEt, microwave, 170 °C, 2 h; (e) Pd(PPh<sub>3</sub>)<sub>4</sub>, RB(OH)<sub>2</sub>, microwave, 165 °C, 20 min.

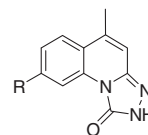
**Table 1**  
SAR for select 4-methyl-7-substituted aryltriazolones

Compd	R	Chk1 IC <sub>50</sub> (μm)
4a		0.19
4b		<0.1
5		0.52
6		0.01
7		0.03
8		0.09
9		1.59
10		0.06
11		0.04
12		0.05
13		0.21
14		0.02
15		0.1
16		76.8
17		24.4

IC<sub>50</sub> values are mean values of three determinations.  
All compounds found to inactive in cellular assay.

ranged from fourfold in the case of 4-acetamido (**13**) to about 40-fold for 4-ethylcarboxamide (**14**).

Additional exploration of the SAR centered on the methylene spaced analogs containing cyclic as well as acyclic amines (**18**–

**Table 2**  
SAR for select 4-methyl-7-substituted aryltriazolones with methylene spacer

Compd	R	Chk1 IC <sub>50</sub> (μm)
18		0.006
19		0.007
20		0.009
21		0.009
22		0.04
23		0.21
24		3.49
25		0.04
26		0.01
27		0.69

IC<sub>50</sub> values are mean values of three determinations.  
All compounds found to inactive in cellular assay.

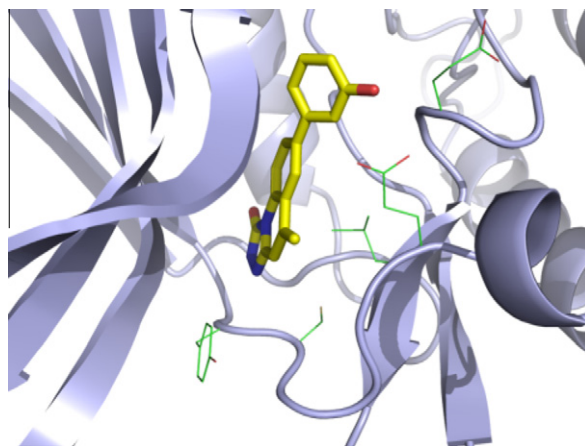
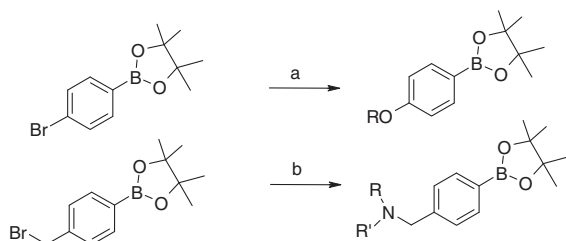


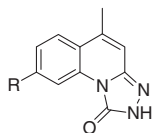
**Figure 3.** Crystal structure of **4a**. In the kinase domain of Chk-1. The canonical interactions observed with **3** are maintained and the 6-substituent phenol is directed in the vicinity of the sugar pocket as originally designed (PDB 2x8i). Picture created using PYMOL.<sup>13</sup>

**21**). The acyclic amine **22** showed ~39 nM potency, but of note are the cyclic variants (**18**–**21**), which showed an approximate 10-fold boost in potency ranging from 6 to 9 nM and were more than two orders of magnitude more potent than the parent triazolone **3**. The Suzuki coupling reaction highlighted in *Scheme 1* was used to prepare examples from commercially available boronic acids. For those



**Scheme 2.** Synthesis of derivatized boronate esters. Reagents and conditions: (a) alkyl chloride (RCl, 1.1 equiv), Cs<sub>2</sub>CO<sub>3</sub> (1.1 equiv), DMF; (b) RR'NH amine, THF (2 M), reflux, 2 h to overnight.

**Table 3**  
4-Methyl-7-heterocyclic triazolones



Compd	R	Chk1 IC <sub>50</sub> (μM)	Abrogation EC <sub>50</sub> (μM)
28		0.014	100
29		0.12	52
30		1.59	N.A.
31		2.96	N.A.
32		0.02	2
33		0.06	13
34		0.0001	0.51
35		0.026	1.5
36		0.004	0.44
37		0.16	3.8
38		0.01	14
39		1.6	1.6

N.A., not available.

IC<sub>50</sub> and EC<sub>50</sub> values are mean values of three determinations.

analogs (**4**, **5**, and **18–21**) where the desired boronic acids were not commercially available, alkylation using the appropriate alkyl chloride or amination of 4-bromomethylphenylboronic acid with the appropriately protected amine was carried out to generate the desired boronate ester prior to conducting the Suzuki coupling and followed by subsequent deprotection as depicted in **Scheme 2**.

Some key matched pairs included the *p*-hydroxymethylphenyl analog (**26**) and its truncated version (**4**) showing 60-fold boosts in potency. This, however, was not a consistent effect, for example, inserting a methylene spacer in the case of **24**, proved to be detri-

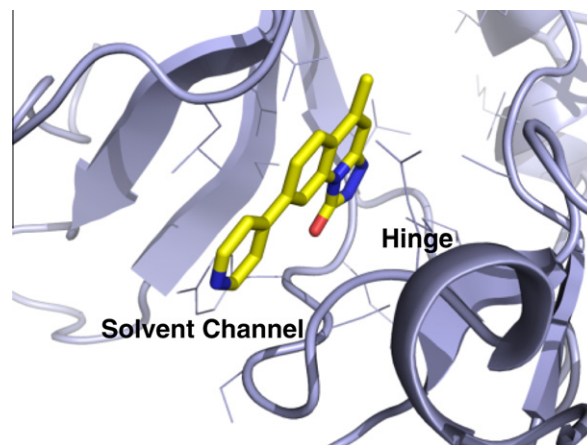


**Figure 4.** The crystal structure of **28**. Bound to the kinase domain of Chk-1. The binding mode differs to those of **3** and **xx** with the core now making H-bonds to the backbone NH of C87 and the backbone carbonyl of C87. The 7-substituent pyridyl is directed down the solvent channel (PDB ID 2x8d). Picture created using PYMOL.<sup>13</sup>

mental and resulted in a decrease in potency from 80 nM (**5**) to 3.4 μM (**24**). The corresponding *m*- and *o*-substituted hydroxymethylphenyl analogs (**25** and **26**) suggest that both the *p*- and *m*-hydroxymethylphenyl substituents are favored over the *o*-hydroxymethylphenyl isomer (**27**).

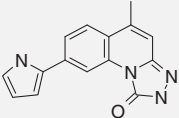
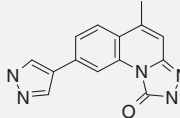
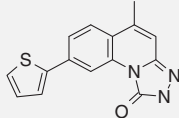
To demonstrate their mechanism of action, Chk1 inhibitors were profiled in a cellular assay where HT29 tumor cells were pre-treated with the DNA damaging agent, camptothecin for 2 h, resulting in cell cycle arrest at G<sub>2</sub>/M. The ability of a compound to abrogate this cell cycle arrest is then quantified by measuring levels of phosphohistone-H3 (a marker of mitosis (M phase)).<sup>2</sup> Although compounds listed in **Tables 1** and **2** were very potent in the Chk1 enzyme assay, they failed to abrogate the G<sub>2</sub>/M block (EC<sub>50</sub> > 12.5 μM). Thus, while successfully generating low nanometer leads at the enzyme level, the reason for the lack of activity in the cellular assay was not clear. Possible explanations investigated were lack of cell permeability, efflux potential, or off-target activity against other kinases, which could potentially mask the cellular phenotype, specifically CDK1.<sup>12</sup> This was found not to be the case as confirmed by screening the compounds in a CDK1 enzyme assay, and we were ultimately unable to determine the precise reason(s) behind the lack of cellular activity for these analogs.

Additional SAR studies were focused on 7-heterocyclic substituted analogs, initially based on commercially available heterocyclic boronic acids.

The design goal for compounds **28–39** was to access either the conserved lysine (Lys<sup>38</sup>) or the P-loop of the Chk1 protein. As summarized by the examples shown in **Table 3**, the 7-heterocyclic substituted triazolone library contained a number of potent compounds. Chk1 enzyme activity revealed that six-membered heterocyclic analogs were generally less potent than five-membered heterocycles with the exception of the 4-pyridyl compound (**28**). Within the subset of five-membered heterocyclic triazolones, a range of activities was observed. The thiazole substituent in **31** was associated with an appreciable loss of potency of 2.96 μM. In contrast, 2 and 3 furanyl substituted analogs, **38** and **39**, respectively, had activity in the low nanomolar range. A striking difference was observed in the activities of 2- and 3-substituted pyrroles, **34** and **35**, respectively, where the former was significantly more potent (0.1 nM) than the latter (26 nM). 2-Pyrazole substitution yielded a 41 nM compound as exemplified by **36**.

Examples **34** and **36** were the most potent inhibitors at the enzyme level, and also led to the abrogation of camptothecin-induced G<sub>2</sub>/M arrest (EC<sub>50</sub> 500 and 440 nM, respectively), consistent with

**Table 4**  
4-Methyl-7-heterocyclic triazolones

			
<i>Physical properties</i>			
log <i>D</i>	3.3	2.1	2.67
Solubility (μM)	2.84	2.83	0.4
PPB (% free)	3	1.3	N.A.
<i>PK properties</i>			
Mouse C1 (ml/min/kg)	68	101	60
<i>T</i> <sub>1/2</sub> (h)	2	0.6	1.3
<i>V</i> <sub>ss</sub> (l/kg)	2.4	5	3.5
<i>Safety</i>			
hERG	>31.6		
<i>Kinase selectivity*</i>			
CDK1 (μM)	46.9	0.24	>100

\* CDK1 kinase routinely checked for all the relevant Chk1 inhibitors in the series. Additional selectivity against a panel of kinases done internally as well as externally as needed to find compound **34** was exquisitely selective against all the kinases tested.

Chk1 inhibition. The positional isomer **35** of pyrrole **34** was found to be threefold less potent at 1.5 μM. Interestingly, the furan matched pairs, while potent in the enzyme assay, showed no G2/M checkpoint abrogation. While the enzyme to cellular potency drop off remained large, a subset of 7-heterosubstituted triazolones were identified which had both enzyme and cellular activity that differentiates them from the aryl-substituted analogs described in Tables 1 and 2. Activity at CDK1 was at first suspected for such a drop off as it may have counterproductive effect on the cellular abrogation.<sup>12</sup> It was ruled out by screening these compounds against CDK1 enzyme assay. The other reasons for such drop off are still being understood but can be speculated to be related to permeability, efflux or other off-target activity.

Compound **28** was co-crystallized with Chk1 enzyme<sup>8</sup> to gain insight into its binding mode. Interestingly, 4-pyridyl moiety bearing **28**, which was originally designed to access Lys<sup>38</sup>, exhibited a different binding mode with respect to **3** and **4a**. The presence of the 4-pyridyl ring led **28** to flip over and position itself in the solvent channel of kinase domain of the protein (Fig. 4). There is a concomitant switching of the interactions between the ligand and the hinge residues with the carbonyl now accepting a hydrogen from the backbone NH of Cys<sup>87</sup> and the NH of the triazolone ring acting as a donor to the backbone carbonyl of Glu<sup>85</sup>. This is in contrast to the aryl group in this position as exemplified by the co-crystal structure of **4a** with Chk1 protein.

Structure guided SAR efforts undertaken towards the TZ class of inhibitors led to the identification of three key compounds listed in Table 4.

To summarize, inhibition of Chk1 is an attractive strategy for identifying anti-cancer therapeutics due to the chemo-potentiating effects obtained when a Chk1 inhibitor is combined with a DNA damaging agent. We have identified a novel series of triazolones from a HTS campaign against Chk1. Utilizing data generated by an initial library campaign, we were able to efficiently improve the potency of a HTS hit from 800 to ~0.1 nM in the Chk1 SPA assay and successfully address limitations of the early analogs, which were devoid of cellular activity. Thus a hit to lead campaign successfully yielded compounds with improved potency (enzymatic and cellular) that were suitable for further lead optimization to generate a Chk1 inhibitor with the desired drug like properties. Since the aspiration was to deliver the Chk1 inhibitor as an intravenous agent, in addition to improving pk, potency, and in vivo efficacy, improving solubility was a key objective of the lead opti-

mization phase of the program, and will be described in the near future.

## Acknowledgments

The authors thank Anne White and Graham Walker for their respective work on the development and implementation of the high-throughput Chk1 kinase screening assay. The authors also thank Elizabeth Mouchet for the development of the cellular abrogation assay.

## References and notes

- (a) Bucher, N.; Britten, C. D. *Br. J. Cancer* **2008**, *98*, 523; (b) Luo, Y.; Levenson, J. D. *Expert Rev. Anticancer Ther.* **2005**, *5*, 333, and references cited within.
- (a) Enzyme and cellular assays have been described in detail in a prior publication as referenced in 13; (b) Zabludoff, S.; Deng, C.; Grondine, M.; Sheehy, A.; Ashwell, S.; Caleb, B.; Green, S.; Haye, H.; Horn, C.; Janetka, J.; Liu, D.; Mouchet, E.; Ready, S.; Rosenthal, J.; Queva, C.; Schwartz, G. K.; Taylor, K. J.; Tse, A. N.; Walker, G. E.; White, A. M. *Mol. Cancer Ther.* **2008**, *7*, 9.
- (a) Janetka, J. W.; Ashwell, S.; Zabludoff, S.; Lyne, P. *Curr. Opin. Drug Discovery Dev.* **2007**, *10*, 473; (b) Arrington, K. L.; Dudkin, V. Y. *ChemMedChem* **2007**, *2*, 1571; (c) Tao, Z.-F.; Lin, N.-H. *Anticancer Agents Med. Chem.* **2006**, *6*, 377; (d) Prudhomme, M. *Recent Patents Anti-Cancer Drug Discovery* **2006**, *11*, 55.
- (a) Wang, Q.; Fan, S.; Eastman, A.; Worland, P.; Sausville, E.; O'Connor, P. *J. Natl. Cancer Inst.* **1996**, *88*, 956; (b) Graves, P.; Yu, L.; Schearz, J. *J. Biol. Chem.* **2000**, *275*, 5600; (c) Busby, E.; Leistriz, D.; Abraham, R.; Karnitz, L.; Sarkaria, J. *Cancer Res.* **2000**, *60*, 2108.
- (a) Fernanda, C.; Filgueira de Azevedo, W., Jr. *Curr. Comput. Aided Drug Des.* **2005**, *1*, 53; (b) Komander, D.; Kular, G.; Bain, J.; Elliot, M.; Van Aalten, D. *Biochem. J.* **2003**, *375*, 255; (c) Goekjian, P.; Jirousek, M. *Expert Opin. Invest. Drugs* **2001**, *10*, 2117.
- Janetka, J.; Almeida, L.; Ashwell, S.; Brassil, P.; Daly, K.; Deng, C.; Gero, T.; Glynn, R.; Horn, C.; Ioannidis, S.; Lyne, P.; Newcombe, N.; Oza, V.; Pass, M.; Springer, S.; Su, M.; Toader, D.; Vasbinder, M.; Yu, D.; Yu, Y.; Zabludoff, S. *Bioorg. Med. Chem. Lett.* **2008**, *18*, 4242.
- The Dundee screen was carried out at 10 μM of compound **3**, 5–50 μM of ATP and consisted of 25 kinases.
- Protein and crystals were obtained as follows:* For CHK1(1-289)-6His and CHK1(1-276)-6His, a baculovirus directing expression of was generated using the Bac-to-Bac method from Invitrogen. Protein was expressed in Sf9(1-289) and Hi5(1-276) insect cells infected with high titre baculovirus at an MOI of 1(1-289) and 2(1-276), and cultured in SF900II media (Invitrogen) for 72 h before harvesting by centrifugation and storage of the cell pellets at –80 °C. Protein was purified by ion exchange, immobilized metal affinity, ATP Sepharose, and size exclusion chromatography: frozen cell pellets were lysed by sonication in buffer A (25 mM Tris, pH 8, 500 mM NaCl, 20 mM imidazole, 14 mM β-mercaptoethanol), the lysate was clarified by centrifugation and then applied to a Q Sepharose FF column. The unbound fraction was loaded directly onto a Ni-NTA column which was washed with buffer A and eluted with a linear gradient from buffer A to buffer B (25 mM Tris, pH 8, 500 mM NaCl,

300 mM imidazole, 14 mM  $\beta$ -mercaptoethanol). Fractions from the eluted peak containing CHK1(1-289)-6His or CHK1(1-276)-6His were pooled, dialysed against buffer C (25 mM Tris, pH 7.5, 500 mM NaCl, 0.5 mM EDTA, 5 mM DTT), diluted with 1.5 volumes buffer D (25 mM Tris, pH 7.5, 20 mM  $\text{MgCl}_2$ , 8% glycerol, 5 mM DTT) and loaded onto an ATP Sepharose column. The ATP Sepharose column was washed with buffer E (25 mM Tris, pH 7.5, 200 mM NaCl, 10 mM  $\text{MgCl}_2$ , 5% glycerol, 5 mM DTT) and eluted with buffer F (25 mM Tris, pH 7.5, 500 mM NaCl, 5% glycerol, 5 mM DTT). Peak fractions containing CHK1(1-289)-6His or CHK1(1-276)-6His were pooled and concentrated using a YM10 membrane before loading on a Sephacryl S-200 sizing column pre-equilibrated with buffer F. Peak fractions containing CHK1(1-289)-6His or CHK1(1-276)-6His were pooled and this final product was concentrated using a YM10 membrane. Co-crystals with compounds **3**, **4a**, and **28** were grown by incubating purified protein at 7 mg/ml with 2 mM compound (1% DMSO) on ice for 30 min, and then setting up a hanging-drop vapour diffusion experiment at 293 K. The reservoir solution for compound **3** was 15–17% (w/v) PEG8000, 250 mM ammonium sulfate, 2% (v/v) glycerol and 100 mM sodium cacodylate pH 6.8. The reservoir solution for compound **4a** was 16–22% (w/v) PEG3350, 150 mM ammonium sulfate and 100 mM BES pH 6.5. The reservoir solution for compound **18** was 12–16% (w/v) PEG3350, 100–200 mM ammonium sulfate, 2% (v/v) glycerol and 100 mM sodium cacodylate pH 6.5. The drop was composed of 3  $\mu$ l protein + compound and 3  $\mu$ l reservoir. Crystals were cryoprotected with ethylene glycol (20% v/v) in mother liquor and flash cooled in a cryostream at 100 K. Diffraction data for complex **3** were collected at Daresbury PX9.6 equipped with a ADSC Quantum 4 X-ray detector, using a  $\text{Si}_{111}$  monochromated wavelength of 0.86 Å at 100 K. Diffraction data for complexes **4a** and **28** were collected at DESY beamline X-13 equipped with a MAR165 CCD X-ray detector, using a  $\text{Si}_{111}$  monochromated wavelength of 0.80 Å. Data for all complexes were processed using MOSFLM and SCALA and were reduced using CCP4 software.<sup>14</sup> The structures were solved by molecular replacement using coordinates of the CHK1 kinase domain as a trial model using CCP4 software. Protein and inhibitor were modeled into the electron density using Quanta,<sup>15</sup> COOT,<sup>16</sup> and Flynn.<sup>17</sup> The model was refined using CNX<sup>18</sup> and the CCP4 program Refmac5.<sup>19</sup> Atomic coordinates<sup>20</sup> and structure factors for the CHK complexes with compounds **3**, **4a**, and **28** have been deposited in the Protein Data Bank (2x8d, 28xi, and 2x8e, respectively) together with structure factors and detailed experimental conditions.

9. Unpublished data.
10. Davis, S.; Rauckman, B.; Chan, J.; Roth, B. *J. Med. Chem.* **1989**, *32*, 1936.
11. C6 positional isomers of compounds **20** and **26** were 2.5 and 1.8  $\mu$ M, respectively.
12. Ashwell, S.; Janetka, J.; Zabludoff, S. *Expert Opin. Invest. Drugs* **2008**, *17*, 1331.
13. DeLano, W. L. *The PyMOL Molecular Graphics System*; DeLano Scientific: San Carlos, CA, USA, 2002. <http://www.pymol.org>.
14. CCP4, *Acta Crystallogr., Sect. D* **1994**, *50*, 760–763.
15. QUANTA2000, Accelrys.
16. Coot, A.; Emsley, P.; Cowtan, K. *Acta Crystallogr., Sect. D* **2004**, *60*, 2126.
17. Flynn, version 1.1.1, OpenEye Scientific Software, Inc., Santa Fe, NM, USA, [www.eyesopen.com](http://www.eyesopen.com), 2010.
18. CNX Version 2000.1, Accelrys.
19. Refmac version 5.1.17 Murshudov, G. N.; Vagin, A. A.; Dodson, E. J. *Acta Crystallogr., Sect. D* **1997**, *53*, 240.
20. Crystallographic statistics for the CHK1–compound **3** complex are as follows: space group  $P2_1$ , unit cell 45.2, 65.7, 58.4 Å,  $\beta$  94.6, resolution 37–1.9 Å (2.0–1.9 Å), 25,219 reflections with an overall redundancy of 2.5 (1.9) give 93.8% (64.6) completeness with  $R_{\text{merge}}$  of 10% (23.5%) and mean  $I/\sigma(I)$  of 8.8 (3.0). The final model containing 2249 protein, 352 solvent, and 15 compound atoms has an  $R$ -factor of 16.0% ( $R_{\text{free}}$  using 5% of the data 19.2%). Mean temperature factors for the protein and the ligand are 18 and 23 Å<sup>2</sup>, respectively. Crystallographic statistics for the CHK1–compound **4** complex are as follows: space group  $P2_12_12_1$ , unit cell 41.3, 70.9, 104.2 Å resolution 31–1.92 Å (2.02–1.92 Å), 22,530 reflections with an overall redundancy of 5.8 (5.4) give 94.3 (89.4) completeness with  $R_{\text{merge}}$  of 8.5% (28.9%) and mean  $I/\sigma(I)$  of 14 (5.6). The final model containing 2110 protein, 241 solvent, and 22 compound atoms has an  $R$ -factor of 18.8% ( $R_{\text{free}}$  using 5% of the data 22.4%). Mean temperature factors for the protein and the ligand are 20 and 26 Å<sup>2</sup>, respectively. Crystallographic statistics for the CHK1–compound **18** complex are as follows: space group  $P2_1$ , unit cell 45.1, 65.9, 54.5 Å,  $\beta$  101.7, resolution 16.6–2.50 Å (2.64–2.5 Å), 7559 Reflections with an overall redundancy of 2.6 (1.7) give 72.5% (26.3%) completeness with  $R_{\text{merge}}$  of 11.3% (26.6%) and mean  $I/\sigma(I)$  of 5.4 (2.0). The final model containing 2054 protein, 352 solvent, and 21 compound atoms has an  $R$ -factor of 23.2% ( $R_{\text{free}}$  using 5% of the data 30.9%). Mean temperature factors for the protein and the ligand are 51 and 93 Å<sup>2</sup>, respectively.